

## Emerging Problems in Infectious Diseases

# The controverted therapeutic efficacy of *Allium sativum* and *Artemisia herba-alba* extracts on *Cryptosporidium*-infected mice

Enas Said Elbahaie<sup>1</sup>, Reda Lamei El Gamal<sup>1</sup>, Ghada Mahmoud Fathy<sup>1</sup>, Asmaa Mohammed Farouk Al-Ghandour<sup>1</sup>, Nadia El-Akabawy<sup>2</sup>, Basma Hosny Abd El Hameed<sup>1</sup>, Samah Hassan Yahia<sup>1</sup>

<sup>1</sup> Department of Medical Parasitology, Faculty of Medicine, Zagazig University, Zagazig, Egypt

<sup>2</sup> Department of Medical Histology and Cell Biology, Faculty of Medicine, Zagazig University, Zagazig, Egypt

### Abstract

**Introduction:** Cryptosporidiosis has become an issue of great interest being life-threatening among immunocompromised hosts worldwide. This study explored the curative effect of *Allium sativum* (garlic) and *Artemisia herba-alba* ethanolic extract versus Nitazoxanide drug on both immunocompetent and immunosuppressed-*Cryptosporidium* experimentally-infected mice.

**Methodology:** One hundred male Swiss albino mice were divided into the following groups: (GI) non-infected non-treated group, (GII) infected non-treated group, (GIII) garlic treated group, (GIV) *A. herba-alba* treated group, (GV) Nitazoxanide treated group, each group subdivided into two subgroups (a) Immunocompetent, (b) immunosuppressed. The assessment was performed by parasitological counting of fecal oocysts, histological examination of intestinal tissue, immunological detection of interferon-gamma levels in mice sera, and ultrastructural study by transmission electron microscopy.

**Results:** Garlic and *A. herba-alba* extracts showed a decrease in the mean oocyst counts through all days of follow-up. This was associated with significant up-regulation of interferon-gamma cytokine levels in serum and histological improvement in intestinal tissues of mice compared to control groups and the results were confirmed by transmission electron microscopy. The highest efficacy was obtained by garlic, then by *A. herba-alba* extracts followed by Nitazoxanide treated group; where the immunocompetent groups showed better improvement than immunosuppressed ones.

**Conclusions:** Garlic has a perfect effect as a promising therapeutic agent against Cryptosporidiosis and therefore validates their traditional use in parasitic infections. Accordingly, it may offer a good option for *cryptosporidium* treatment in immunocompromised patients. They could be used as a natural safe product for the preparation of a new therapeutic agent.

**Key words:** *Cryptosporidium*; garlic; artemisia; nitazoxanide; IFN- $\gamma$ ; TEM.

*J Infect Dev Ctries* 2023; 17(6):732-743. doi:10.3855/jidc.0000

(Received 08 September 2022 – Accepted 07 December 2022)

Copyright © 2023 Elbahaie *et al.* This is an open-access article distributed under the Creative Commons Attribution License, which permits unrestricted use, distribution, and reproduction in any medium, provided the original work is properly cited.

### Introduction

*Cryptosporidium* is an opportunistic, enteric protozoan parasite of chief medical importance in clinical practice. The most frequently recognized species infecting humans are *Cryptosporidium parvum* and *Cryptosporidium hominis* [1]. This parasite mainly affects the intestinal epithelium, resulting in gentle to serious acute watery diarrhea that is typically self-settled within two weeks in immunocompetent, but it could be chronic, life-threatening, devastating infection, leading to dehydration, starvation, and even mortal outcome in immunocompromised hosts [2].

Till now, Nitazoxanide (NTZ) is the main FDA-approved therapy for cryptosporidiosis [3], yet it does not work without adequate immunity and showed poor efficacy in immunocompromised hosts [4]. As there is neither an effective vaccine nor therapeutic preventing

or treating such hosts, identification of new remedies is essential. Herbal products received a great reputation and were used as non-conventional antiparasitosis [5].

Garlic (*Allium sativum*) has been used as a medication for millennia in various civilizations. Its medicinal mystical properties were written about on the walls of ancient temples. It has been identified not only as a spice but also as a chemical pharmaceutical agent capable of controlling microbes [6], thus garlic is receiving great attention as a potent antimicrobial and antiparasitic medicinal plant.

*Artemisia herba-alba* plant is a single-stemmed annual weedy herb. The most important bioactive compounds are artemisinin, dihydroartemisinic acid, artemisinic acid, and arteannuin B [7]. Various studies have analyzed the antiparasitic role of artemisinin and its derivatives against several infections like;

cryptosporidiosis, giardiasis, amoebiasis, leishmaniasis, clonorchiasis, malaria, and schistosomiasis [8].

Therefore, this work was performed to determine the therapeutic efficacy of garlic and *A. herba-alba* extracts as compared to the conventional treatment for cryptosporidiosis, NTZ, in experimentally infected immunocompetent and immunosuppressed mice at parasitological, biochemical, histological, and ultrastructural levels.

## Methodology

### Parasite

Stool samples were collected from several immunocompromised individuals with persistent diarrhea at Zagazig University Hospitals' Inpatient Departments. *Cryptosporidium*-positive samples without other parasitic co-infections were preserved in 2.5% potassium dichromate aqueous solution at 4°C until required [9].

### Experimental animals

This study involved 100 healthy laboratory-bred Swiss albino male mice, (20-25 gm; 3- 4 weeks age) provided by Schistosomal Biological Center at Theodor Bilharz Research Institute (TBRI) in Giza, Egypt. All mice were housed in separate cages that were appropriately ventilated. Pelleted food and water were available all over the day [10]. They were cared for in accordance with the research procedures and Animal Experimentation Guidelines established by the National Institutes of Health Ethics committee at Zagazig University's Faculty of Medicine authorized the experimental protocol (Institutional Review Board, IRB, ZU-IRB 4672- (4-6-2018).

### Design of the experiment

Five groups of mice (20 mice each) were created. Each group was then sectioned into two equal subgroups: GIa: Immunocompetent (IC) - free of infection, received no treatment; GIb: Immunosuppressed (IS) - free of infection, received no treatment; GIIa: IC, infected with *Cryptosporidium*, non-treated; GIIb: IS, infected, non-treated mice; GIIIa: IC mice with *Cryptosporidium* infection, and received garlic at a dose of 50mg/kg/day; GIIIb: IS, infected, and treated with the same dose of garlic; GIVa: IC, infected, and treated with *A. herba-alba* (500 mg/kg/day); GIVb: IS mice with *Cryptosporidium* infection which received the same dose of *A. herba-alba*; GVa: IC, infected, and treated with NTZ (100 mg/kg/day); GVb: IS, infected, and treated with NTZ. Treatment regimens were

provided daily via stomach tubes 1 hour before meals beginning on the fifth day after *Cryptosporidium* infection and lasting 5 days in immunocompetent subgroups [11] and 10 days in immunosuppressed ones [12].

### Immunosuppression

For 14 days previous to infection with *Cryptosporidium* oocysts, 0.25 mg/kg/day of synthetic corticosteroid (dexamethasone) manufactured by a local pharmaceutical company in Egypt (Kahira) were taken orally. Throughout the trial and until the completion of the study, the mice received the same dosage of dexamethasone [13].

### Infection

Positive stool samples were diluted with distilled water, filtered, and centrifuged at 2500 rpm for 10 minutes. The supernatant fluid was discarded and the sediment was washed twice in 1 mL of phosphate buffer saline (PBS), with centrifugation at 13,000 rpm for 2 minutes. After repeated washing followed by centrifugation, fecal debris was eliminated [14].

For counting the number of *Cryptosporidium* oocysts in 1mL of the sample, three slides were prepared from the sample; each of them 50µL, stained by MZN stain, and then the mean of three counts of oocysts per high-power field was calculated and multiplied by 20 to get the number in 1000 µL (1mL) [15].

Except for the negative control, prepared inoculums of *Cryptosporidium* oocysts (10<sup>3</sup> oocysts/ mouse) were used to infect the entire examined mice groups through the esophagus using a tuberculin syringe linked to a polythene tube. The mice were inoculated once [16]. This step occurred on the 15<sup>th</sup> day for dexamethasone immunosuppressed groupings [17]. The mice were dehydrated overnight before being implanted orally.

### Plant material

#### Allium sativum (garlic)

Freshly peeled bulbs of garlic were thoroughly rinsed with distilled water. Garlic bulbs were dried before being crushed in a blender. In distilled water, the powder was dissolved to make an aqueous solution of 1 gm/ml concentration. Small aliquots of raw garlic mixture were kept at -20 degrees Celsius until needed [18]. The workable solution was created by diluting the stock one with distilled water. The garlic dosage used in this study was 50 mg/kg/day [19].

### Artemisia herba-alba (Shih)

The dry leaves of the plant were ground by the electric grinder. Before filtering with filter paper, the plant powder was steeped in 70% ethyl alcohol for three days. The revolving evaporator condensed the filtrate under a vacuum. The technique was performed multiple times until the plant materials were utterly depleted. Out of 200 gm dried powder, 55 gm ethanolic extract of *A. herba-alba* was obtained [20]. The dosage chosen for this study was 500 mg/kg/day [21].

### Nitazoxanide

Medizen Pharmaceutical Industries manufactured and supplied Utopia Pharmaceuticals with 500 mg tabs of Nanazoxide. The selected dosage for the present work was 100 mg/kg/day [22].

### Animal scarification

At the end of the research (21st-day post-infection), all mice were killed by quick decapitation. Parts of the intestine from each mouse were removed and subjected to histological and TEM examination. The serum also was subjected to immunological studies.

### Evaluation of the anti-cryptosporidial activity of garlic and *A. herba-alba* extracts

#### Parasitological assessment

From all mice groups, fecal pellets were gathered before and after the treatment schedule at 5<sup>th</sup>, 10<sup>th</sup>, 15<sup>th</sup> & 21<sup>st</sup> dpi, and subjected to parasitological examination to count *Cryptosporidium* oocysts. The oocysts number was expressed per gram of feces [23]. Using the following equation, the effectiveness percentage of each extract was computed.

$$\text{Efficacy percentage} = \frac{m_{pc} - m_t}{m_{pc}} \times 100$$

where:  $m_{pc}$  = mean oocyst count of positive control group;  $m_t$  = mean oocyst count of treated group.

#### Histological light microscopic analysis

After scarification, fine sections from the terminal part of ileum of all mice groups were fixed in formalin 10% and stained with hematoxylin and eosin (H&E) [24]. To determine the number of goblet cells, staining of some sections with Alcian blue was done. The goblet cells were counted on ten non-overlapping fields of villous-crypt units that were randomly chosen for each section at  $\times 400$  magnification (VCU) [25].

#### Transmission electron microscopy (TEM)

Nearly 1 mm<sup>3</sup> of the distal ileum of all mice groups was immediately fixed after scarification in

glutaraldehyde 5% prepared in 0.1 M Sodium Cacodylate solution for 24 hours at 4 °C. Further fixation was accomplished by immersing the samples in Osmium Tetroxide (OSO<sub>4</sub>) 1% in the same buffer for 2 hours at room temperature. Fixed specimens were dehydrated in ascending grades of ethanol before being implanted in epoxy resin. To designate the target region for ultra-structural analysis, stained semi-thin slices with toluidine blue dye were visualized under optical microscopy. As a final step, the cut ultrathin slices were stained with Uranyl acetate and lead citrate [26], before being investigated for ultra-structural changes in the invasive stages of the parasite with a JEOL-JEM 1010 TEM at 80 kV at the Regional Center for Mycology.

#### Determination of interferon-gamma (IFN- $\gamma$ ) level using ELISA

As a final step before ending this experiment, blood samples were withdrawn from the heart under ketamine/xylazine anesthesia (0.1 mL/100g IP) into heparin-free tubes. Blood tubes were left in an upright position at room temperature for 30 minutes then centrifuged at 3000 rpm for 15 min to separate the sera which were aliquoted and stored at -20 °C. Concentrations of IFN- $\gamma$  were assessed by commercially available ELISA Kit after the manufacturer's instructions (Mouse IFN- $\gamma$  ELISA kit, Chongqing Biospes Co., Ltd #BEK1081, Chongqing Shi, CN). At 450 nm filters, the optical density values were estimated. Concentrations of IFN- $\gamma$  were determined from standard curve 31.2-2000 pg/mL assay ranges.

#### Statistical analysis

The obtained information was entered into a computer excel sheet and statistically evaluated with the Statistical Package for Social Science program version 27.0 [27]. All data was provided as mean  $\pm$  SD. "One-way ANOVA" was utilized for the distinction between quantitative variables between more than two groups, while the repeated measure ANOVA test was utilized for the same group for many periods. A  $p$  value  $< 0.01$  was considered extremely statistically significant,  $p < 0.05$  was considered significant, and  $p > 0.05$  was considered insignificant.

## **Results**

### Parasitological results

Oocysts of *C. parvum* were identified in the fecal samples of the infection groups (Figure 1). On the 21<sup>st</sup> dpi; comparing the mean oocyst counts in 1 gm stool of immunocompetent and immunosuppressed mice

groups, there were highly statistically significant differences between mean oocyst counts on all days of follow-up ( $p < 0.01$ ) in all treated groups. The percentage of oocysts reduction was 82.65%, 50.92%, and 73.9% in GIIIa, GIVa, and GVa groups, respectively. Moreover, the percentage of oocysts reduction was 72.38%, 33.21%, and 50.50% in GIIIb, GIVb, and GVb groups, respectively. Furthermore, with the passage of follow-up time, the percentage of oocyst reduction increased across the various groups of infected mice (Tables 1 and 2). Garlic therapy resulted in the highest percentage of reduction in oocyst counts 82.65%, while the *A. herba-alba* treated group showed the lowest percentage of reduction 50.92%.

**Histological light microscopic results**

Examination of hematoxylin and eosin-stained sections in the ileum of the non-infected, non-treated groups revealed normal villous architecture with preserved brush border (Figure 2a), while those of infected, untreated groups showed a broadening of the villi, areas of lost brush border, superficial ulcerations (Figure 2b). Moreover, sub-epithelial villous edema and inflammatory cellular infiltrations were noted plus several areas of dysplasia in the form of nuclear stratification. *Cryptosporidium* oocysts were also seen attached to the brush border (Figure 2c). After treatment with garlic, the best results were reported, and there was a restoration of the normal architecture of the majority of the sections compared to infected and untreated

groups, especially among IC mice. However, limited areas of villous edema and inflammatory cellular infiltrates were seen beside the attached *Cryptosporidium* oocyst (Figure 2d, 2e). After *A. herba-alba* treatment, mice showed minimal improvement in the histological structure, changes were similar to the infected untreated control groups with different degrees of dysplastic changes, villous edema, and submucosal inflammatory cellular infiltrates (Figure 2f). In IS *A. herba-alba* treated mice, the improvement in the histological structure was less, and intraepithelial lymphocytic infiltrations were obvious (Figure 2g). After NTZ treatment, mild improvement in the histological picture was noted.

**Figure 1.** Cryptosporidium oocysts (arrow) in stool samples stained by MZN ( $\times 1000$ ).

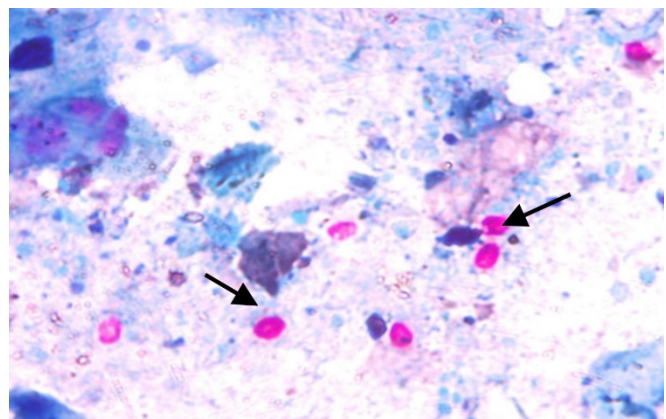


**Table 1.** Comparison of mean oocyst counts in 1gm stool in the immunocompetent mice subgroups at various follow-up time points.

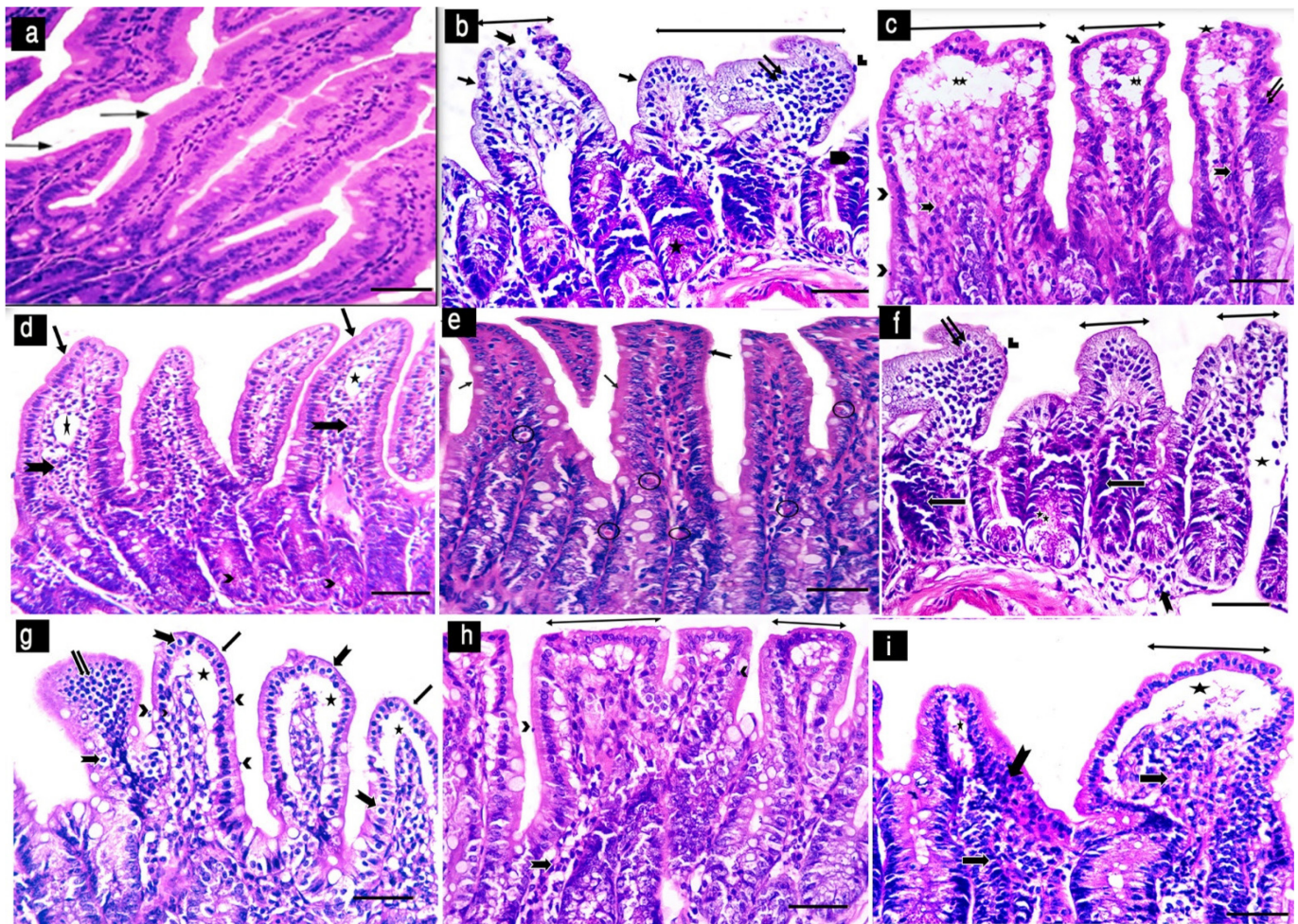
Group	$(\bar{x} \pm SD) \times 10^3$ Percentage of reduction				F <sup>^</sup>	p value
	5 <sup>th</sup> dpi	10 <sup>th</sup> dpi	15 <sup>th</sup> dpi	21 <sup>st</sup> dpi		
Gla	--	--	--	--		
GIIa	93.8 $\pm$ 3.77	89.7 $\pm$ 2.83 a	83.33 $\pm$ 2.92 a	78.56 $\pm$ 2.13 a	30.08	0.01*
GIIIa	93.8 $\pm$ 3.77	44.6 $\pm$ 4.55 b, 50.28%	30.5 $\pm$ 4.7 b, 63.4%	13.7 $\pm$ 3.27 b, 82.65%	557.69	< 0.001**
GIVa	94 $\pm$ 3.77	65.4 $\pm$ 4.99 c, 27.09%	51.22 $\pm$ 2.54 c, 38.53%	38.56 $\pm$ 3.75 c, 50.92%	749.83	< 0.001**
GVa	94.4 $\pm$ 3.17	49.5 $\pm$ 5.62 b, 44.82%	35.9 $\pm$ 3.45 d, 56.92%	20.5 $\pm$ 4.35 d, 73.9%	402.07	< 0.001**
F	0.06	193.51	421.05	647.5		
P	0.98 NS	< 0.001**	< 0.001**	< 0.001**		

**Table 2.** Comparison of mean oocyst counts in 1gm stool in the immunosuppressed mice subgroups at various follow-up time points.

Group	$(\bar{x} \pm SD) \times 10^3$ Percentage of reduction				F <sup>^</sup>	p value
	5 <sup>th</sup> dpi	10 <sup>th</sup> dpi	15 <sup>th</sup> dpi	21 <sup>st</sup> dpi		
GIIb	--	--	--	--		
GIIIb	219.1 $\pm$ 5.43	224.13 $\pm$ 5.59 a	222.29 $\pm$ 5.82 a	218.43 $\pm$ 3.95 a	26.58	0.004*
GIVb	219.8 $\pm$ 4.05	127.33 $\pm$ 4 b, 43.19%	96.56 $\pm$ 3.81 b, 56.56%	60.33 $\pm$ 4.72 b, 72.38%	3517.59	< 0.001**
GIVb	222.2 $\pm$ 5.37	178 $\pm$ 5.29 c, 20.58%	163 $\pm$ 6.74 c, 26.6%	145.88 $\pm$ 5.49 c, 33.21%	149.30	< 0.001**
GVb	222 $\pm$ 5.66	149.4 $\pm$ 3.24 d, 33.34%	127.25 $\pm$ 5.15 d, 42.75%	108.13 $\pm$ 5.62 d, 50.50%	496.15	< 0.001**
F	0.91	718.78	767.48	1382.02		
P	0.46 NS	< 0.001**	< 0.001**	< 0.001**		

SD: Standard deviation; F: ANOVA test; F<sup>^</sup>: Repeated measure ANOVA test; \*: significant ( $p < 0.05$ ); \*\*: highly significant ( $p < 0.001$ ); NS: nonsignificant ( $p > 0.05$ ). Groups with different letters are statistically significant ( $p < 0.05$ ); Common letters are statistically non-significant ( $p > 0.05$ ).

**Figure 2.** Hematoxylin and eosin-stained sections in intestinal tissue showing: (a) non-infected control groups: normal villous architecture with normal preserved brush border (arrow). In IC infected not treated group (b), the villi appear broad (double head arrow) with areas of lost brush border (arrow) and superficial ulcerations (notched arrow) beside *Cryptosporidium* oocysts that are seen attached to the brush border (arrowhead). hyperchromatic nuclei (pentagon), nuclear stratification (double arrows) and eosinophilic stained Paneth cells (star) are also noticed. In IS-infected not treated group (c), wide broad villi (double head arrow) appear with loss of the brush border (arrow), ulcerations (star), sub-epithelial villous edema (double stars), and attached *Cryptosporidium* oocysts (arrowhead). Nuclear stratification (double arrows) with inflammatory cellular infiltration in the lamina propria (notched arrow) are obvious. In the IC garlic treated group (d), villi/crypt pattern is normal (arrow), and some villi show edema (star). Inflammatory cells infiltrate the lamina propria (notched arrow) and eosinophilic stained Paneth cells are seen at the base of the crypts (arrowhead). In IS garlic-treated group (e), normal villi/crypt pattern appears with preserved brush border (arrow), and lamina propria shows eosinophilic inflammatory infiltration (circle). In IC Artemisia treated group (f), villi are broad (double head arrow) with dysplastic changes in the form of hyperchromatic nuclei (arrow) and nuclear stratification (double arrows). *Cryptosporidium* oocyst is noticed attached to the brush border (arrowhead) with underlying villous edema (star) and submucosal inflammatory cellular infiltrates (notched arrow). Paneth cells are obvious at the base of the crypts (double stars). In IS Artemisia treated group (g), many areas with lost brush border (arrow) and nuclear stratification (double arrows). Intraepithelial lymphocytic infiltration (notched arrow) and sub-epithelial villous edema are marked (star). *Cryptosporidium* oocysts are attached to the brush border (arrowhead). IC NTZ treated group (h), shows broad villi (double head arrow) and marked submucosal inflammatory cellular infiltration (notched arrow). *Cryptosporidium* oocysts are attached to the brush border (arrowhead). In IS NTZ treated group (i), villi are broad (double head arrow) with marked sub-epithelial villous edema (star). Nuclear stratification and hyperchromatism are observed (notched arrow). Inflammatory cellular infiltration is seen all over the lamina propria (arrow). [H&E, Scale bar = 50µm].



Many villi were short and broad with areas of luminal epithelial cell desquamation, sub-epithelial villous edema, inflammatory cellular infiltration, and dysplastic changes, especially in IS mice (Figure 2h, 2i).

Alcian blue-stained sections showed an average number of Alcian blue positive goblet cells in the non-infected non-treated groups (Figure 3a, 4). In infected non-treated groups, Alcian blue positive goblet cells were very few, even some villi demonstrated areas of total goblet cells depletion (Figure 3b). In garlic-treated groups, goblet cells were abundant, and the droplets were fully filled with the stain and scattered all over the length of the villi and crypts (Figure 3c). In *A. herba-alba* treated groups, goblet cells were moderate in number with many areas of goblet cell depletion (Figure 3d). In NTZ-treated groups, numerous goblet cells were variable in size and scattered all over the length of the villi and crypts (Figure 3e).

*Transmission Electron Microscopic (TEM) results*

The TEM examination of ultrathin sections of the small intestinal epithelial cells in GI revealed absorptive columnar cells with numerous apical microvilli. Each cell contains oval euchromatic nuclei, and abundant mitochondria, in addition to well-developed cell junctions in between. Goblet cells were visualized studded with plenty of mucous granules of

moderate electron density (Figure 5a). After infection induction to GII group, the ultrastructure of the small intestine in IC mice (GIIa) showed lost apical microvilli, degenerated epithelial cells with rarified cytoplasm, pyknotic nuclei, degenerated organelles, and several multivesicular bodies (Figure 5b). In addition, the ultrastructure of IS mice (GIIb) showed macrogametes between microvilli that were enveloped by a parasitophorous vacuole. The cytoplasm of macrogametes contained many polysaccharide granules and rough endoplasmic reticulum.

**Figure 4.** Percentage of goblet cells number in Alcian blue-stained sections in all the study groups.

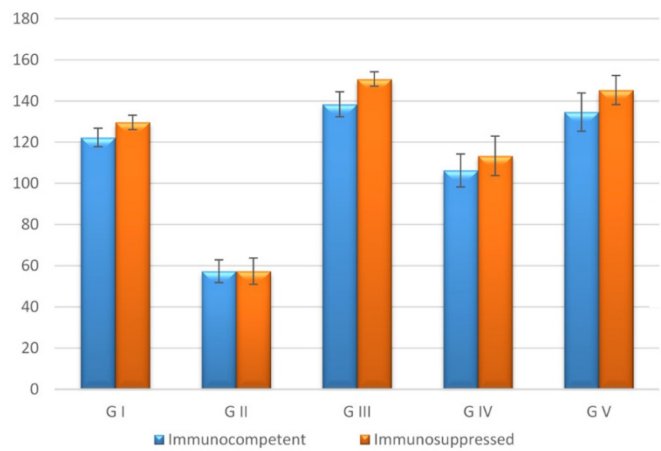


**Figure 3.** Alcian blue-stained intestinal sections showing: (a) In the non-infected control groups, average number of Alcian blue positive goblet cells (arrow). The colored droplets are variable in size and scattered all over the length of the villi and crypts. (b) In infected not treated groups, very few Alcian blue positive goblet cells (arrowhead). Some villi show areas of total goblet cell depletion (arrow). (c) In garlic treated groups, abundant Alcian blue positive goblet cells (arrow). The droplets are fully filled with the stain and scattered all over the length of the villi and crypts. (d) In artemisia treated groups, moderate number of Alcian blue positive goblet cells (arrow) with many areas of goblet cells depletion (arrowhead). (e) In NTZ treated groups, numerous Alcian blue positive goblet cells (arrow). The colored droplets are variable in size and scattered all over the length of the villi and crypts. [Alcian blue, Scale bar = 50µm].

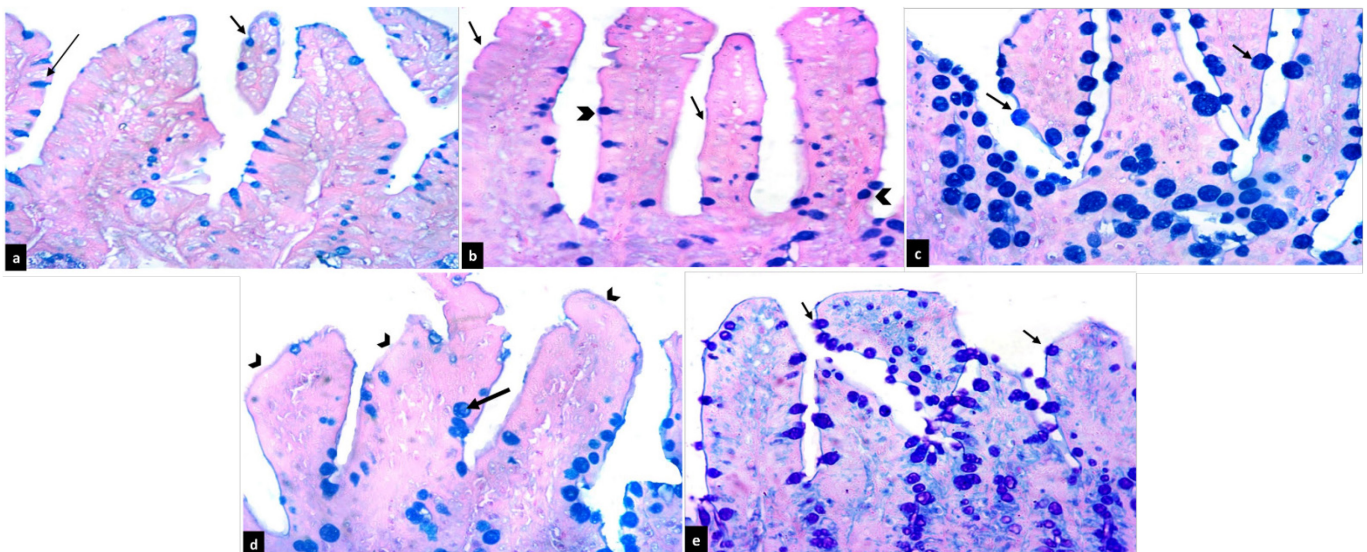
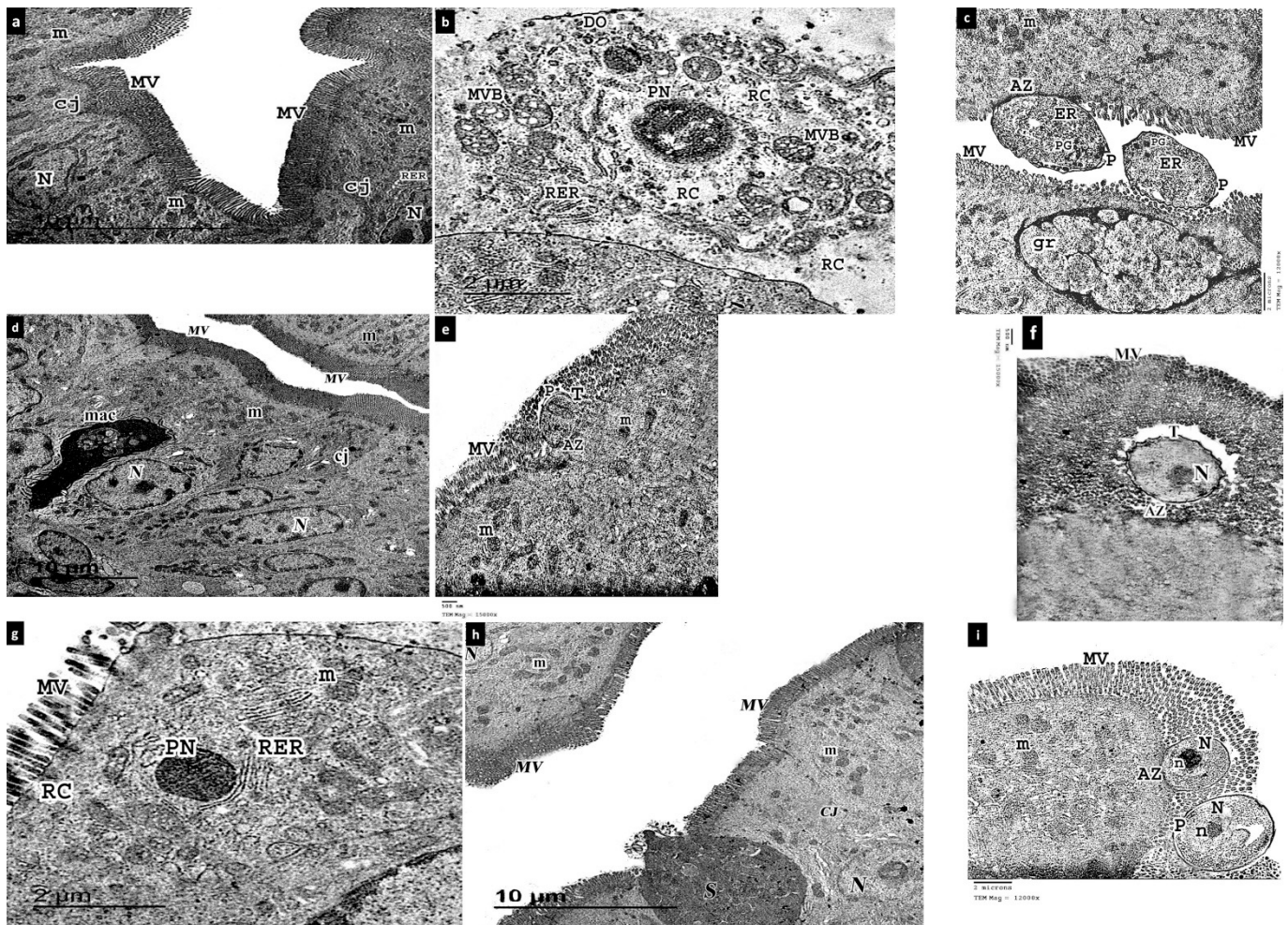


**Figure 5.** Transmission electron micrographs of sections in the small intestine showing; (a) non-infected control groups, intestinal columnar epithelial cells with prominent microvilli (mv) and regular euchromatic nuclei (N), plentiful mitochondria (m), rough endoplasmic reticulum (RER) and well-developed cell junctions (cj). (b) In IC infected not treated group, lost apical microvilli and even apical cell membrane (arrow), degenerated epithelial cells with rarified cytoplasm (RC), pycnotic nucleus (PN) and degenerated organelles (DO). Several multivesicular bodies (MBV) and rough endoplasmic reticulum (RER) are seen. (c) IS infected not treated group, 2 macrogametes (arrows) present between microvilli (MV) and enveloped by a parasitophorous vacuole (P), the cytoplasm of both macrogametes contains many polysaccharide granules (PG) and rough endoplasmic reticulum (ER), the attachment zone (AZ) is obvious at the base of the upper one only. Goblet cell is seen containing mucous granules of moderate electron density (gr). The columnar epithelial cells contain multiple swollen mitochondria (m). (d) IC garlic treated group, the absorptive columnar cells appear with numerous apical microvilli (mv), plentiful mitochondria (m), regular oval euchromatic nuclei (N), and well-developed cell junctions (cj). Macrophage (mac) with prominent pseudopodia (arrow) is seen in between. (e) IS garlic treated group, Cryptosporidium trophozoite (T) is incarcerated between apical microvilli (MV) and completely covered with the double-layered membrane derived from the microvilli; the parasitophorous vacuole (P), the parasite pellicle forms a feeder organelle at the attachment zone (AZ). The enterocytes are full of swollen mitochondria (m). (f) IC artemisia treated group, Cryptosporidium trophozoite (T) is incarcerated in between the apical microvilli (MV) with its characteristic nucleus (N) and a double membrane pellicle (arrows). The attachment zone (AZ) is not yet fully formed. (g) IS artemisia treated group, microvilli (mv) appear distorted with manifestations of cellular degeneration; rarified cytoplasm (RC), pycnotic nucleus (PN), swollen mitochondria (m), cell membrane blebbing (arrow), and well-demarcated outer limiting membrane (arrowhead). Multiple cisternae of rough endoplasmic reticulum (RER) are seen. (h) IC NTZ treated group, regularly arranged apical microvilli (mv) with oval euchromatic nuclei (N), plentiful mitochondria (m) and well-developed cell junctions (cj). Atypical goblet cell appears with electron-dense condensed secretion (S). Part of the mucus is seen extravasating into the intestinal lumen (arrow). (i) IS NTZ treated group, distorted apical microvilli (MV) with two trophozoites embedded in between, the characteristic nuclei (N) and prominent nucleoli (n) are seen within. The attachment zone (AZ) is obvious in the upper trophozoite and the parasitophorous vacuole (P) is prominent in the lower one. Swollen mitochondria (m) are plentiful.



Goblet cells were also seen containing mucous granules of moderate electron density. The columnar epithelial cells appeared with multiple swollen mitochondria (Figure 5c). Evident changes were noticed in the overall cellular ultrastructure and cytoplasm of the luminal trophozoites treated with garlic (GIII) when compared to the infected non-treated group (Figure 5d, 5e). *Cryptosporidium* trophozoite appeared incarcerated in between the microvilli with near normalization of the villi architecture. After *A. herba-alba* administration (GIV), deformed trophozoites were seen with altered intestinal cells ultrastructure, especially in IS mice. The intestinal cells showed distorted microvilli, cellular degeneration, pycnotic nuclei, and swollen mitochondria (Figure 5f, 5g). In GV group, NTZ- treated mice showed different degrees of deviation from the normal ultrastructure. Some intestinal cells showed normal columnar epithelial cells with numerous apical microvilli, regular oval euchromatic nuclei, and plentiful mitochondria, others showed distorted microvilli and swollen mitochondria especially among IS mice (Figure 5h, 5i).

#### Determination of interferon-gamma (IFN- $\gamma$ ) level using ELISA

ELISA analysis of serum IFN- $\gamma$  revealed a significantly substantial rise in all treated groups ( $p < 0.01$ ) when compared to the non-treated infected groups. Nevertheless, its level in all immunosuppressed groups was lower than the corresponding immunocompetent ones (Figure 6).

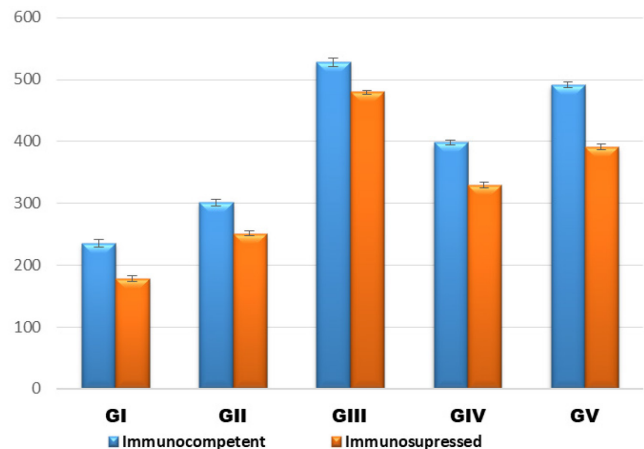
## Discussion

*Cryptosporidium* infection is considered the second driving reason of infectious diarrheal illnesses in developing countries that could possess a fatal outcome, mostly in children and immunosuppressed patients [28]. There is no satisfactory treatment for cryptosporidiosis, therefore, searching for an alternate effective therapy is a worthy research topic.

In the present study, both garlic and *A. herba-alba* extracts were assessed in the treatment of cryptosporidiosis, as a potential replacement for the already used chemotherapeutic drug "NTZ" for all mice groups. The chemical suppression of immunity in immunosuppressed subgroups increases the susceptibility to *Cryptosporidium* infection.

In this study, garlic herbal extract was found to be the most effective therapy against cryptosporidiosis. On the 21<sup>st</sup> day of treatment, the therapeutic outcome of garlic on cryptosporidiosis was statistically significant in both IC and IS mice subgroups which agrees to some

**Figure 6.** Serum IFN- $\gamma$  level among both IC and IS mice subgroups.



extent with studies that show garlic successfully eradicates the oocysts from the feces of experimentally infected mice [29]. Additionally, Fareed *et al.* [30] reported that *Allium sativum* was utilized to treat cryptosporidiosis in HIV patients suffering persistent diarrhea, with complete recovery in some and partial healing in others. Several mechanisms could explain garlic's success in the treatment of experimental cryptosporidiosis. It enhances phagocytic activity of natural killer cells with subsequent improvement of the host immunity against infection. Garlic also inhibits some regular activities of the parasite, like food absorption, motility, and replication, according to Azimi *et al.* [31]. On the other hand, one study from Iraq reported a lower efficacy of garlic against *Cryptosporidium* infection due to the suboptimal used dose [21]. So, the effectiveness of garlic increases with increasing doses of plant extracts.

On the 21<sup>st</sup> day of the study, *A. herba-alba* exhibited a statistically significant effect on *Cryptosporidium* infected mice which was in line with the results of Al-Hamairy *et al.* [21] as well as Majeed *et al.* [32], who found *A. herba-alba* to have antiprotozoal action against *C. parvum* oocyst shedding in infected mice. The active artemisinin and santonin in Artemisia may be the reason for its potency, it prevents *Cryptosporidium* oocysts from penetrating cells and protects against cellular damage [33].

The impact of NTZ on cryptosporidiosis-infected mice was statistically significant on the 21<sup>st</sup> day of treatment. These findings are nearly comparable to those of Amadi *et al.* [34], who observed cessation of diarrhea in HIV-free patients after nitazoxanide treatment, but with no significant parasitological effect in HIV-infected patients. Madbouly *et al.* [35] recorded

a 52.7% decrease in oocyst shedding in experimentally infected immunosuppressed mice treated with NTZ at 21<sup>st</sup> dpi. However, Mostafa *et al.* [36] exhibited a very low reduction rate, about 8.2% at 21<sup>st</sup> dpi in immunosuppressed infected mice treated with NTZ. These disparities could be attributed to variations in the doses, drug formulations, and the used animal models.

In our study, the histological sections were evaluated to assess the structural alterations associated with *cryptosporidium* infection. Marked alterations in the small intestinal sections in infected untreated mice groups were also seen. These findings were in line with Madbouly *et al.* [35], who revealed that cryptosporidiosis pathological changes varied from limited to total villous atrophy with heavy cellular infiltrates. The justification for these findings was attributed to the ability of the parasite to dislodge the brush borders, producing an asymmetric loss of the epithelial cells, resulting in shorter villi, fusing, and broadening. Villous atrophy was explained by the direct damage to the epithelial cells via the secreted toxins. Cellular atrophy and fluffing due to edema in the lamina propria induced by the infection, along with mucosal inflammation, can result in reduced fluid, water, and electrolyte absorption in the gut [37].

Hyperplasia is usually thought to indicate an attempt to rebuild the destroyed villus epithelium induced by microbes, and it also contributes to immunity by releasing antimicrobial peptides to protect against the invading pathogen [38]. The IC subgroups showed a satisfying degree of histological structural corrections compared to the IS groups which agreed with Moawad *et al.* [15].

The garlic-treated mice group demonstrated a significant improvement in the villi architecture. The significant improvement due to garlic use can be explained by the restoration of the brush border to its original form, even in areas where the parasite was still attached, as well as a rise in the number of Paneth cells performing a defensive role of antibody production against microbes [39].

*A. herba-alba* treated mice group showed limited improvement in the histological picture, Majeed *et al.* [32] reported significant improvement in intestinal histopathology after *A. herba-alba* treatment. *A. herba-alba* has been used as a cytoprotective agent for gastric ulcers and assumed that its active principle, dehydroleucodine, increased gastric glycoproteins synthesis and prevented gastric mucosa lesions [40].

Nitazoxanide-treated mice group showed mild improvement with the restoration of some villi and crypts architecture compared to the infected non-treated

groups, although some sections showed detached irregular villi, cellular infiltration, edema, and fewer *C. parvum* oocysts. This was consistent with the findings of Sadek and El-Aswad [12] who found that NTZ had moderate efficacy against *C. parvum* infection.

Paneth cells were detected with their characteristic granules at the base of the crypts in immunocompetent mice groups and reduced in immunosuppressed ones which agreed with Kelly *et al.* [41], who showed fewer Paneth cells in HIV-infected patients with *Cryptosporidium* because of a decrease in the granule content of terminally developed Paneth cells. These cells are thought to regulate microbial density in the small intestine lumen by preventing penetration into the crypt microenvironment [42].

Regarding Alcian-blue staining, the number of goblet cells decreased within the infected sections and this agreed with Maruyama *et al.* [43], who reported the loss of goblet cells plus some absorbent cells that appeared in the form of empty vacuoles in *Cryptosporidium* infection. On the other hand, hyperplasia of goblet cells could occur due to cryptosporidiosis infection playing a key role in the production of antimicrobial agents [39]. We could attribute this discrepancy to the severity and stage of infection. A strongly positive reaction in infected groups was explained by the presence of high secretions of sulfamic and sialomucine which act as magnificent protectors against *Cryptosporidium* infection [44]. Those mucins are highly hydrophilic and can bind water to form a gel-like structure, preventing direct contact between enterocytes and the intraluminal content, especially pathogenic microorganisms [45].

In the current work, the count of goblet cells increased in all treated groups as compared to the non-treated infected group. These findings were agreed with Oshiba *et al.* [46], who documented the improvement in the local immune response in the intestinal mucosa after NTZ treatment and increased the number of goblet cells. They added that goblet cells play a vital role in local humoral immunity by anti-microbial antibodies production. Moreover, goblet cells maintain intestinal homeostasis as they establish intimate interactions with gut immune cells [47].

In the present work, TEM was done to investigate the underlying ultra-structural alterations responsible for the light microscopic histological findings. The histopathological alterations found in the infected, non-treated groups (GII) matched with Ayabe *et al.* [42] and Fawzy *et al.* [48]. Variable degrees of microvilli regeneration and restoration of normal architecture with different stages of the parasite were identified in the

treated groups. The garlic-treated group improved significantly, with a picture similar to the control groups. The NTZ-treated group showed moderate improvement in villous architecture, while *A. herba alba*-treated group showed very limited improvement. *Cryptosporidium* trophozoites were observed incarcerated in between the microvilli with shortening of the adjacent microvilli. The structure of the trophozoites were matched with the findings of Sanad *et al.* [49].

IFN- $\gamma$  is the most important cytokine in the battle against *Cryptosporidium* because it stimulates Th1 cytokine production such as nitric oxide, reactive oxygen species, in addition to antimicrobial peptides. All of which inhibit intracellular parasite growth [50]. In the current study, the serum level of IFN- $\gamma$  cytokine increased significantly in GII-infected mice. This is consistent with Abouel-Nour *et al.* [51] and El-Sayed and Fathy, [52], who reported a significant rise in the level of all circulating cytokines in *Cryptosporidium* infected mice compared to control mice. Opposite observation of relatively low levels of serum IFN- $\gamma$  in the immunocompromised infected mice in comparison to normal control non-infected have been obtained by other researchers [3,53].

In comparison with the negative control group, all of our treated mice subgroups, particularly the immunocompetent ones, showed a substantial rise in IFN- $\gamma$  serum levels. This rise is directed against *Cryptosporidiosis* establishment. These observations come in accordance with Sanad *et al.* [49], and Al-Ghandour *et al.* [53], who found that protection against this parasite has been largely concomitant with the production of IFN- $\gamma$ . The level of IFN- $\gamma$  was higher in the immunocompetent than in the corresponding immunosuppressed ones which is in agreement with the finding of Farid *et al.* [54].

## Conclusions

The highest efficacy was obtained by garlic, then by *Artemisia* herbal extracts followed by Nitazoxanide treated group; where the immunocompetent groups showed better improvement than immunosuppressed ones. Garlic has a perfect effect as a promising therapeutic agent against *Cryptosporidiosis* and therefore validates their traditional use in parasitic infections. Accordingly, it may offer a good option for *cryptosporidium* treatment in immunocompromised patients. They could be used as a natural safe product for the preparation of a new therapeutic agent.

## Authors' contributions

Reda Lamei El gamal conceptualized the idea. Asmaa Mohammed Farouk Al-Ghandour, Ghada Mahmoud Fathy, and Basma Hosny Abd El hameed performed the study design and material preparation. All authors shared in the laboratory work. Nadia El- Akabawy assessed the histological and TEM results. The principal draft of the manuscript was written by Enas S. Elbahaie and Basma Hosny Abd El hameed and all authors commented of preceding versions of the manuscript. All authors read and approved the final manuscript.

## References

1. Khan A, Shaik JS, Grigg ME (2018) Genomics and molecular epidemiology of *Cryptosporidium* species. *Acta Trop* 184: 1-14. doi: 10.1016/j.actatropica.2017.10.023.
2. Zhang G, Zhang Y, Niu Z, Wang C, Xie F (2020) *Cryptosporidium parvum* upregulates miR-942-5p expression in HCT-8 cells via TLR2/TLR4-NF-kB signaling. *Parasit Vectors* 13: 435-439. doi: 10.1186/s13071-020-04312-x.
3. El-Wakil ES, Salem AE, Al-Ghandour AMF (2020) Evaluation of possible prophylactic and therapeutic effect of mefloquine on experimental cryptosporidiosis in immunocompromised mice. *J Parasit Dis* 45: 380-393. doi: 10.1007/s12639-020-01315-4.
4. Fahmy A, Fahmy Z, Aly E, Elshenawy A, ELWakil E (2021) Therapeutic potential of Commiphora molmol extract loaded on chitosan nanofibers against experimental cryptosporidiosis. *PUJ* 14: 39-45. doi: 10.21608/puj.2021.55537.1102.
5. Capela R, Moreira R, Francisca Lopes F (2019) An overview of drug resistance in protozoal diseases. *Int J Mol Sci* 20: 5748. doi: 10.3390/ijms20225748.
6. Abed HH, Yakoob AY (2013) Study the protective and therapeutic effects of crude garlic on mortality, oocyst output and hepatic lesions in experimental infection with *Eimeria stiedae* in domestic rabbits. *Basrah J Vet Res* 12: 314-331. doi: 10.33762/bvetr.2013.83827.
7. Ferreira JFS, Janick J (1995) Production and detection of artemisinin from *Artemisia annua*. *Acta Horticulturae* 390: 41-49. doi: 10.17660/ActaHortic.1995.390.5.
8. Ataei AA, Delnavaz HB (2019) Terpenoid compounds and anti-hemozoin and anti-ciliates protozoans effects of *Artemisia annua* L. and *Chenopodium botrys*. *L J Med Plants* 18: 49-66. doi: 10.29252/jmp.3.71.49.
9. Abbassi H, Wyers M, Cabaret J, Naciri M (2000) Rapid detection and quantification of *Cryptosporidium baileyi* oocysts in feces and organs of chickens using a microscopic slide flotation method. *Parasitol Res* 86: 179-187. doi: 10.1007/s004360050029.
10. El-Fakhry Y, Achbarou A, Desportes I, Mazier D (1998) *Encephalitozoon intestinalis*: humoral responses in interferon- $\gamma$  receptor knockout mice infected with a *Microsporidium* pathogenic in AIDS patients. *Exp Parasitol* 89: 113-121. doi: 10.1006/expr.1998.4267.
11. Aboelsoued DM, Shaapan RM, Ekhateeb RMM, Elnattat WS, Abd elhameed MF, Hammam AMM, Hammam A (2020) Therapeutic efficacy of ginger (*Zingiber officinale*), ginseng (*Panax ginseng*) and sage (*Salvia officinalis*) against *Cryptosporidium parvum* in experimentally infected mice. *Egypt J Vet Sci* 51: 241-251. doi: 10.21608/ejvs.2020.24183.1152.

12. Sadek GS, El-Aswad BE (2014) Role of COX-2 in pathogenesis of intestinal cryptosporidiosis and effect of some drugs on treatment of infection. *Res J Parasitol* 9: 21-40. doi: 10.3923/jp.2014.21.40.
13. Rehg JE, Hancock ML, Woodmansee DB (1988) Characterization of a dexamethasone-treated rat model of cryptosporidial infection. *J Infect Dis* 158: 1406 - 1407. doi: 10.1093/infdis/158.6.1406.
14. Garcia LS and Bruckner DA (1997) Macroscopic and microscopic examination of fecal specimens. *Diagnostic Medical Parasitology* (3rd ed.), AMS press, Washington DC. P: 608-649.
15. Moawad HS, Hegab MH, Badawey MS, Ashoush SE, Ibrahim SM, Ali AAS (2021) Assessment of chitosan nanoparticles in improving the efficacy of nitazoxanide on cryptosporidiosis in immunosuppressed and immunocompetent murine models. *J Parasit Dis* 45: 606-619. doi: 10.1007/s12639-020-01337-y.
16. Moon HW, Schwartz A, Welch MJ, McCann PP, Runnels PL (1982) Experimental fecal transmission of human cryptosporidia to pigs, and attempted treatment with an ornithine decarboxylase inhibitor. *Vet Pathol* 19: 700-707. doi: 10.1177/030098588201900615.
17. Riad NHA, Taha HA, Mahmoud YI (2009) Effects of garlic on albino mice experimentally infected with *Schistosoma mansoni*: A parasitological and ultrastructural study. *Trop Biomed* 26: 40-50.
18. Burke JM, Wells A, Casey P, Miller JE (2009) Garlic and papaya lack control over gastrointestinal nematodes in goats and lambs. *Vet Parasitol* 159:171. doi: 10.1016/j.vetpar.2008.10.021.
19. Masamba B, Gadzirayi CT, Mukutirwa I (2010) Efficacy of *Allium sativum* (garlic) in controlling nematode parasites in sheep. *J Appl Res Vet Med* 8: 161-169.
20. Abdallah HMI, Abdel-Rahman RF, Abdel-Jaleel GA, Abd El-Kader H A M, El-Marasy S A, Zaki E R, Bashandy SAE, Arbid MS, Farrag AH (2015) Pharmacological effects of ethanol extract of *Artemisia Herba Alba* in streptozotocin-induced type 1 diabetes mellitus in rats. *Biochem Pharmacol* 4: 1-13. doi: 10.4172/2167-0501.1000196.
21. Al-Hamairy AK, Mugheer AH, Al-Dulaim FHA (2012) Prevalence of *Cryptosporidium* sp. and treatment by using some plant extracts in al-hilla city, Babylon province of Iraq. *Egypt J Exp Biol Zool* 8: 287 - 293.
22. Li X, Brasseur P, Agnamey P, Leméteil D, Favennec L, Ballet JJ, Rossignol JF (2003) Long-lasting anticryptosporidial activity of nitazoxanide in an immunosuppressed rat model. *Folia Parasitol* 50: 19-22. doi: 10.14411/fp.2003.003.
23. Benamrouz S, Guyot K, Gazzola S, Mouray A, Chassat T, Delaire B, Chabé M, Gosset P, Viscogliosi E, Dei-Cas E, Creusy C, Conseil V, Certad G (2012) *Cryptosporidium parvum* infection in SCID mice infected with only one oocyst: qPCR assessment of parasite replication in tissues and development of digestive cancer. *PLoS One* 7: 512-532. doi: 10.1371/journal.pone.0051232.
24. Drury RAB, Wallington EA (1980) In Carleton's Histological technique. 4th ed. Oxford Univ. Press, New York, Toronto. 36-125.
25. Allen A, Hutton DA, Leonard AJ, Pearson JP, Sellers LA (1986) The role of mucus in the protection of the gastroduodenal mucosa. *Scand J Gastroenterol Suppl* 125: 71-78. doi: 10.3109/00365528609093820.
26. Al-Mathal EM, Alsalem AM (2012) Pomegranate (*Punica granatum*) peel is effective in a murine model of experimental *Cryptosporidium parvum*. *Exp Parasitol* 131: 350-357. doi: 10.1016/j.exppara.2012.04.021.
27. IBM corp. Released (2020) IBM SPSS statistics for windows, Version 27.0. Armonk, NY: IBM corp.
28. Gebretsadik D, Metaferia Y, Seid A, Fenta G M, Gedefie A (2018) Prevalence of intestinal parasitic infection among children under 5 years of age at dessie referral hospital: Cross sectional study. *BMC Res Notes* 11: 771. doi: 10.1186/s13104-018-3888-2.
29. Abdel Megeed KN, Hammam AM, Morsy GH, Khalil FAM, Seliem MME, Aboelsoued D (2015) Control of cryptosporidiosis in buffalo calves using garlic (*Allium sativum*) and nitazoxanide with special reference to some biochemical parameters. *Glob Vet* 14: 646-655.
30. Fareed G, Scolaro M, Jordan W, Sanders N, Chesson C, Slattery M, Long D, Castro C (1996) The use of a high-dose garlic preparation for the treatment of *Cryptosporidium parvum* diarrhea. *Int. Conf. AIDS* 11: 288.
31. Azimi H, Fallah-Tafti M, Karimi-Darimiyan M, Abdollahi M (2011) A comprehensive review of vaginitis phytotherapy. *Pak J Biol Sci* 14: 960-966. doi: 10.3923/pjbs.2011.960.966.
32. Majeed SA, Al-Taai NA, Al-Zubaidi IA (2015) The effect of aqueous alcohol *Artemisia herba-alba* and *Thymus vulgaris* extract on the *Cryptosporidium parvum* in the white mouse (BALB/C). *Int J Adv Res* 3: 31-35.
33. Brisibe EA, Umoren UE, Owai PU, Brisibe F (2008) Dietary inclusion of dried *Artemisia annua* leaves for management of coccidiosis and growth enhancement in chickens. *African J Biotechnology* 7: 4083-4092.
34. Amadi B, Mwiya M, Musuku J, Watuka A, Sianongo S, Ayoub A, Kelly P (2002) Effect of nitazoxanide on morbidity and mortality in zambian children with cryptosporidiosis: a randomised controlled trial. *Lancet* 360: 1375-1380. doi: 10.1016/S0140-6736(02)11401-2.
35. Madbouly NT, Hebat SA, Yousof HA, El-Sayed S H, Younis A I, Mohamed SJ (2017) Atorvastatin repurposing for the treatment of cryptosporidiosis in experimentally immunosuppressed mice. *Exp Parasitol* 181: 57-69. doi: 10.1016/j.exppara.2017.07.010.
36. Mostafa NE, Abdel Hamed EF, Fawzy EM, Zalat RS, Rashed HE, Mohamed SY (2018) The new trend in the treatment of experimental cryptosporidiosis and the resulting intestinal dysplasia. *Colorectal Cancer* 7: 1758-1958. doi: 10.2217/crc-2018-0008.
37. Zadrozny LM, Stauffer SH, Armstrong MU, Jones SL, Gookin JL (2006) Neutrophils do not mediate the pathophysiological sequelae of *Cryptosporidium parvum* infection in neonatal piglets. *Infect Immun* 74: 5497-5505. doi: 10.1128/IAI.00153-06.
38. Tarver AP, Clark DP, Diamond G, Russell JP, Erdjument-Bromage H, Tempst P, Cohen KS, Jones DE, Sweeney RW, Wines M, Hwang S, Bevins CL (1998) Enteric  $\beta$ -defensin: molecular cloning and characterization of a gene with inducible intestinal epithelial cell expression associated with *Cryptosporidium parvum* Infection. *Infect Immun* 66: 1045-1056. doi: 10.1128/IAI.66.3.1045-1056.1998.
39. Bourlioux P, Koletzko B, Guarner F, Braesco V (2003) The intestine and its microflora are partners for the protection of the host: report on the Danone Symposium "The Intelligent Intestine", held in Paris *Am J Clin Nutr* 78: 675-683. doi: 10.1093/ajcn/78.4.675.
40. Derakhshanfar A, Oloumi MM, Kabootari J, Arab H (2006) Histopathological and biomechanical study on the effect of

- Artemisia sieberi extract on experimental skin wound healing in rat. *Iran J Vet Surg* 1: 36-42.
41. Kelly P, Feakins R, Domizio P, Murphy J, Bevins C, Wilson J, Mcphail G, Poulosom R, Dhaliwal W (2004) Paneth cell granule depletion in the human small intestine under infective and nutritional stress. *Clin Exp Immunol* 135: 303-309. doi: 10.1111/j.1365-2249.2004.02374.x.
  42. Ayabe T, Satchell DP, Wilson CL, Parks WC, Selsted ME, Ouellette AJ (2000) Secretion of microbicidal alphadefensins by intestinal paneth cells in response to bacteria *Nat Immunol* 1: 113-118. doi: 10.1038/77783.
  43. Maruyama H, Tanaka M, Hashimoto M, Inoue M, Sasahara T (2007) The suppressive effect of Mekabu fucoidan on an attachment of *Cryptosporidium parvum* oocysts to the intestinal epithelial cells in neonatal mice. *Life Sci* 80: 775-781. doi: 10.1016/j.lfs.2006.11.020.
  44. Al-Kennany ER, Rahawi AM, Al-Jabori SA (2012) Histopathological and histochemical study of intestinal cryptosporidiosis in mice. *Kufa Jou. Vete. Med. Sci.* 3.
  45. Birchenough GM, Johansson ME, Gustafsson JK, Bergström JH, Hansson GC (2015) New developments in goblet cell mucus secretion and function. *Mucosal Immunol* 8: 712-719. doi: 10.1038/mi.2015.32.
  46. Oshiba SF, Yasein RI, El-Shennawy AM, Aiad HA, El-Wakil EA (2018) In vivo effect of pomegranate (*Punica granatum*) extracts versus nitazoxanide drug on the ileum of experimentally infected mice with *Cryptosporidium parvum* oocysts. *J Am Sci* 14.
  47. Yang S, Yu M (2021): Role of goblet cells in intestinal barrier and mucosal immunity. *J Inflamm. Res* 14: 3171-3183. doi: 10.2147/JIR.S318327.
  48. Fawzy EM, Zalut RS, Rashed HE, Salama MA, Saleh AA, Abdelamed EF (2019) Effect of cinnamon and ginger methanolic extracts on murine intestinal cryptosporidiosis. in-vivo evaluation *J Egypt Soc Parasitol* 49: 689- 698. doi: 10.21608/jesp.2019.68076.
  49. Sanad MM, Al-Malki JS, Al-Ghabban AG (2015) Control of cryptosporidiosis by probiotic bacteria. *AEMS* 7-8.
  50. Hunter CA, Sibley LD (2012) Modulation of innate immunity by *Toxoplasma gondii* virulence effectors. *Nat Rev Microbiol* 10: 766-778. doi: 10.1038/nrmicro2858.
  51. Abouel-Nour MF, El-Shewehy DMM, Hamada SF, Morsy TA (2015) The efficacy of three medicinal plants: garlic, ginger and mirazid and a chemical drug metronidazole against *Cryptosporidium parvum*. I-Immunological response. *J Egypt Soc Parasitol* 45: 559-70. doi: 10.21608/jesp.2015.96295.
  52. El-Sayed NM, Fathy GM (2019) Prophylactic and therapeutic treatments' effect of *Moringa oleifera* methanol extract on *Cryptosporidium* infection in immunosuppressed mice. *Antiinfect Agents* 17: 130-137. doi: 10.2174/2211352517666181221094420.
  53. Al-Ghandour AM, Yousef AM, Mohamed RM, Tealeb AM, Ahmed HK, Atwa HA, Farag TI (2020) Prophylactic anticryptosporidial activity of atorvastatin versus nitazoxanide on experimentally infected immunosuppressed murine models. *J Egypt Soc Parasitol* 50: 535-546. doi: 10.21608/jesp.2020.131084.
  54. Farid A, Tawfik A, Elsioufy B, Safwat G (2021) In vitro and in vivo anti-*Cryptosporidium* and anti-inflammatory effects of Aloe vera gel in dexamethasone immunosuppressed mice. *Int J Parasitol Drugs Drug Resist* 17: 156-167. doi: 10.1016/j.ijpddr.2021.09.002.

#### Corresponding author

Enas S. El-Bahaie, MD  
Lecturer of Medical Parasitology  
Faculty of Medicine, Zagazig University  
City of Zagazig, Sharqiyyah Governorate, 44511, Egypt  
Tel: +20 1275326558  
Email: enas.elbahaie@gmail.com

**Conflict of interests:** No conflict of interests is declared.